Industrial Engineering Journal
ISSN: 0970-2555
Volume : 52, Issue 12, No. 3, December : 2023

STUDY THE CONSEQUENCE OF RASTER ANGLE ON THE CHARPY IMPACT STRENGTH OF FDP 3D PRINTED POLYLACTIC ACID MESOSTRUCTURE

Dr. B. Sambi Reddy, Associate Professor, Department of Mechanical Engineering, NIST (Autonomous), Berhampur, 761008, Odisha, India.
E-mail: bsreddy.design@gmail.com; bsreddy@nist.edu;

Abstract
Polylactic acid (PLA) is a versatile polymer utilized in fused deposition modeling (FDM) 3D printing due to its biodegradable and biocompatible properties. PLA's limited impact strength restricts its use in structural and functional components. This study examined the impact of raster angle on the Charpy impact strength of 3D printed PLA mesostructure. The impact strength of PLA specimens with various raster angles (0°, 15°, 30°, 45°, 60°, 75°, and 90°) was measured using a Charpy impact tester. The study involved analyzing the impact energy absorption, notched impact strength, and analysis fracture surfaces of the specimens through microscopy. The results found that the impact strength of PLA mesostructure decreased as the raster angle increased from 0° to 90°. The impact strength was highest at a 0° raster angle, showing a 29% increase compared to the 90° raster angle. The analysis of fractography provided insights into the mechanisms of fracture and the propagation of cracks. The findings indicate that the angle of the raster plays a crucial role in influencing the impact behavior of FDM 3D printed PLA mesostructure. It is possible to choose an ideal raster angle to improve the impact strength of PLA mesostructure.

Keywords: PLA, 3D printing, Raster Angle, Charpy impact test, Notched impact strength, Fractography.

Graphical Abstract:

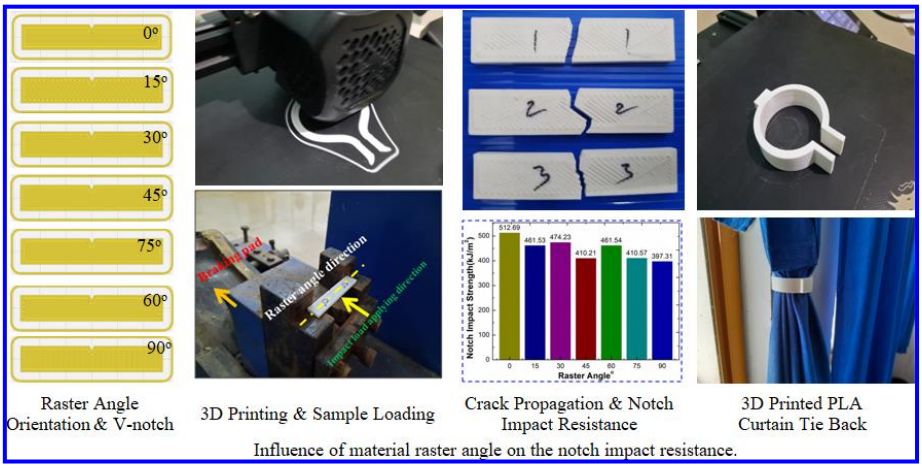

Introduction

Additive manufacturing (AM) refers to a manufacturing technique whereby three-dimensional (3D) objectives are produced by sequentially depositing layers of material in accordance with a digital model. AM has several benefits in comparison to traditional production techniques, including enhanced design freedom, increased customization capabilities, less material waste, and expedited prototype processes [**1-3**]. FDM is a very prevalent and easily accessible process within the realm of AM, namely for the production of polymer-based components. The FDM technique involves the use of a heated nozzle to extrude a thermoplastic filament onto a build platform, therefore progressively constructing the intended shape in a layer-by-layer manner [**4-5**]. On the other hand, PLA is a polymer with biodegradable and biocompatible properties, often used as a printing medium in FDM processes.

PLA has favorable mechanical characteristics, including notable tensile strength and modulus, when juxtaposed with other thermoplastic materials [**6-7**]. Nevertheless, it is important to acknowledge that PLA does possess some limitations that must be taken into consideration. These include its relatively low impact strength, thermal stability, and ductility, which therefore restrict its potential uses in both structural and functional components [**8-9**]. Hence, enhancing the impact strength of PLA components fabricated by FDM is a significant area of investigation in research.

The mechanical characteristics of FDM-printed components may be influenced by several variables, one of which is the raster angle. The raster angle refers to the angle formed between the printing direction and the longitudinal axis of the part [**10-11**]. The orientation and alignment of printed layers and filaments, as determined by the raster angle, have a significant impact on the strength of interlayer and interfiber bonding. The stress distribution and fracture mechanism of the printed component under loading are also influenced by the raster angle [**12-13**]. Hence, the optimization of the raster angle in FDM-printed PLA components has the potential to improve their impact strength and overall performance.

According to research, the raster angle has a considerable effect on the impact strength of FDM-printed PLA pieces. Rajpurohit and Dave [**14**] discovered that the greatest impact strength was obtained using a 0° raster angle, 300 m layer height, and 700 m raster width. Furthermore, when the raster angle grew from 0° to 45°, the fracture mode shifted from brittle to ductile. This emphasizes the need of considering raster angles when developing FDM-printed products. Syrlybayev et al. [**15**] investigated the optimization of FDM-printed component strength qualities utilizing a variety of factors such as infill density, infill patterns, extrusion temperature, layer thickness, nozzle diameter, raster angle, and build orientation. They identified layer thickness as the most important element and proposed that pre-processing with laser or infrared heating may improve interlayer bonding. Lanzotti et al. [**16**] investigated the influence of raster angle, layer height, and shell perimeter number on the tensile stress of 3D printer manufactured PLA samples. From the outcome, it discovered that by reducing layer height and increasing the number of shell perimeters enhanced tensile stress. Furthermore, diagonal raster angles had better tensile stress than horizontal or vertical raster angle of samples. Wang et al. [**17**] used 3D printing to produce PLA honeycomb structures and investigated the effect of raster angle on mechanical properties and fracture behaviour. It was discovered that as the raster angle increased from 0° to 45°, the compressive stress and modulus of structure increased, and subsequently decreased as the raster angle increased to 92°. Furthermore, when the raster angle grew from 0° to 45°, the behavior changed from brittle to ductile, and additional raster angle samples displayed brittle behavior. Mechanical characteristics and failure mechanism of 3D-printed PLA lattice structures were studied by Zhang et al. [**18**]. They found that the PLA lattice structures' compressive strength and modulus enhanced from 0° to 45° of raster angle, and subsequently decreased when the raster angle was raised to 90 degrees. The failure mechanism of lattice structures' shifted from local buckling to global buckling when the raster angle went from 0° to 90°. Liu et al. [**19**] found that the PLA cellular structures' compressive strength and modulus improved from 0° to 45° of raster angle, but decreased from 45° to 90° of raster angle. With an increase in raster angle from 0° to 90°, the cellular structures' fracture morphology changed from interlayer delamination to interfiber debonding. Mishra et al. [**20**] investigated the effect of infill density (10% to 100%) and patterns (namely, zig-zag, concentric circles, honeycomb, grid, and triangular, etc.) on the impact strength of 3D printed PLA samples. From the results, it found that 85% infill density and line pattern sample shown highest impact energy absorbing capabilities.

The primary aim of this study is to investigate the effect of raster angle on the impact resistance of PLA samples that are developed employing FDM technique. The present study included the development and production of PLA samples with different raster angles (0°, 15°, 30°, 45°, 60°, 75°, and 90°). Subsequently, the specimens were evaluated for notched impact strength using a Charpy impact tester. Furthermore, the fracture surfaces of the samples were analyzed by the use of microscopy.

Industrial Engineering Journal
ISSN: 0970-2555
Volume : 52, Issue 12, No. 3, December : 2023

Material and Methods

Design and printing of samples

The 3D model of the Charpy impact sample was produced using the CREO-1.0 parametric solid modeling program, according to the ASTM D256 design guidelines (Figure 1). A selection of 21 specimens was made, including various raster angles (Table 1). The specimens were produced via the 'Creality Ender 3 V2' 3D printer, employing the Fused Deposition Modeling (FDM) method and utilizing PLA material. The appropriate process parameters, as outlined in Table 2, were used during fabrication.

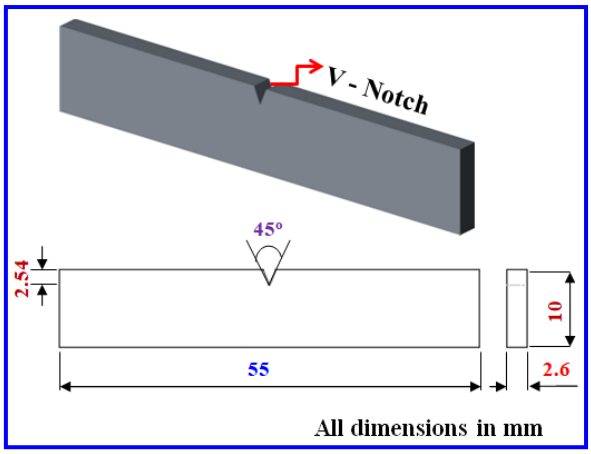

Figure 1: V-notch impact testing sample 3D model developed and geometrical properties are represented as per the ASTM D 256.

Table 1: Impact test specimens are having different infill raster angles with respect to longitudinal axis of specimen.

Sl. No.	Infill Raster Angle	Number of Samples
1	0°	3
2	15°	3
3	30°	3
4	45°	3
5	60°	3
6	75°	3
7	90°	3

Table 2: Constant process parameters for 3D printing

Sl. No.	Printing parameters	Values	units
1	Layer height	0.2	mm
2	Initial layer height	0.2	mm
3	Line width	0.35	mm
4	Wall line width	0.35	mm
5	Outer wall line width	0.35	mm
6	Inner wall line width	0.3	mm
7	Wall thickness	1	mm
8	Wall line count	3	---
9	Printing Temperature	200	°C
10	Build plate temperature	60	°C
11	Nozzle flow	100	%
12	Build plate adhesion type	None	---

Experimental setup

Each sample set consisted of three specimens for a given group of process parameters. The results were taken as the average impact strength values of the mechanical test. In order to account for the potential variability of physical characteristics in various materials a series of tests were performed at room temperature in accordance with established norms. The research included the performance of Charpy impact tests to examine the energy absorption capabilities and determine the specific kind of damage shown by various configurations. The Charpy impact strength test is a commonly used ASTM procedure for evaluating the impact resistance of materials. A pivoting arm, which has a constant potential energy, as seen in Figure 2, is elevated to a predetermined height and thereafter released. The arm descends, subsequently making impact with a grooved specimen, resulting in the fracture of such specimen. The determination of the energy absorbed by the sample is based on the measurement of the height at which the arm swings when it comes into contact with the sample. The total impact energy of fracture = mg (H-h) -- J**.** In the context, the variables m, g, H, and h represent the mass, acceleration due to gravity, initial height, and ultimate height, respectively. The impact strength, denoted as the absorbed energy per unit cross-sectional area (expressed in kJ/m2), may be calculated using the formula: Impact strength = (impact energy / (width x thickness)). The energy losses resulting from bearing friction and air resistance were disregarded owing to their very little impact on the overall energy balance.

The Charpy tests were performed using Impact equipment, using a 13.5 kg head hammer that strikes the sample at a velocity of 3.5 m/s. The specimen is properly positioned inside the sample holder, ensuring that the notch of the sample is precisely aligned with the impact load line of action. In addition, a hand brake mechanism was used to regulate and return the hammer to a state of rest, as seen in Figure 2. In order to generate potential energy inside the hammer, the hammer was elevated to an angle of 150^{o} relative to the sample plane. The location of impact is situated on the opposing side of the notch sample, so facilitating the process of crack propagation (see Figure 4).

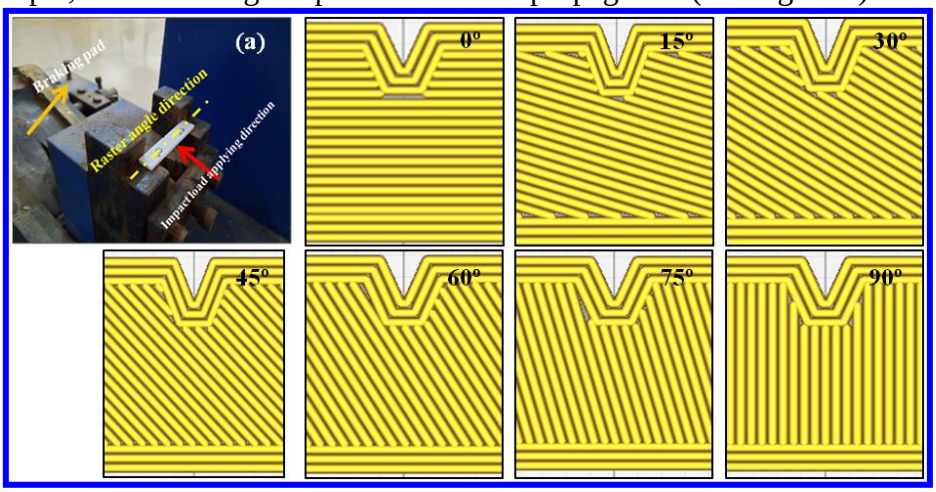

Figure 2: (a) Sample loading on Charpy impact testing rig and samples infill raster angle (0^{o} to 90^{o}) with respect to longitudinal axis.

Results and Discussion

The Charpy impact test was performed on 3D printed PLA specimens of varying raster angles to assess their notch impact strength and examine the phenomenon of crack propagation. The outcome revealed that PLA demonstrated a certain degree of impact toughness, but it was vulnerable to brittle fracture when subjected to impact loading. Additionally, the investigation involved a comprehensive fractography analysis of the fractured samples. This investigation unveiled the fracture surface's characteristics, such as crack initiations, crack propagation patterns, and the extent of brittle and ductile behavior. These outcomes provide important insights into the fracture mechanics of 3D printed samples; assist in material selection and product design for applications where impact resistance is a

fundamental consideration. Furthermore, research and optimization of PLA's mechanical properties with respect to the raster angle can enhance its performance in a range of engineering applications.

Energy Absorption and Notch Impact strength of PLA

The findings from the impact test carried out with PLA specimens produced by 3D printing, which had different raster angles, provide significant insights into the influence of layer orientation on energy absorption in the context of impact occurrences, as shown in Figure 3a. As per the analysis of Figure 3a, it observed that there are fluctuations in energy absorption when the material raster angle changes from 0^o to 90^o. The impact energy absorption varied from 10.33 J to 13.33 J. The PLA specimen, when oriented with a raster angle of 0°, exhibits the maximum energy absorption of 13.33 J. This finding implies that, in the context of this particular scenario, aligning the printing layers perpendicular to the impact direction yields optimal energy absorption capabilities. Upon doing data analysis, it becomes evident that some raster angles, namely 15°, 30°, and 60°, demonstrate a notable degree of consistency in terms of energy absorption levels, which around 12 J. Nevertheless, when considering raster angles of 45°, 75°, and 90°, it is seen that the energy absorption values are relatively lower, ranging from around 10.33 J to 10.78 J. The available data indicates a significant correlation between the angle of the raster and the absorption of energy. It seems that raster angles in close proximity to 0° exhibit enhanced energy absorption capabilities, while angles that deviate farther from 0° lead to decreased energy absorption.

In summary, the findings of the impact test demonstrate the significant effect of raster angle on the capacity of PLA samples to absorb energy. The research suggests that a raster angle of 0° results in the greatest energy absorption. However, it is important to take into account the individual applications and impact resistance requirements when deciding on the appropriate raster angle.

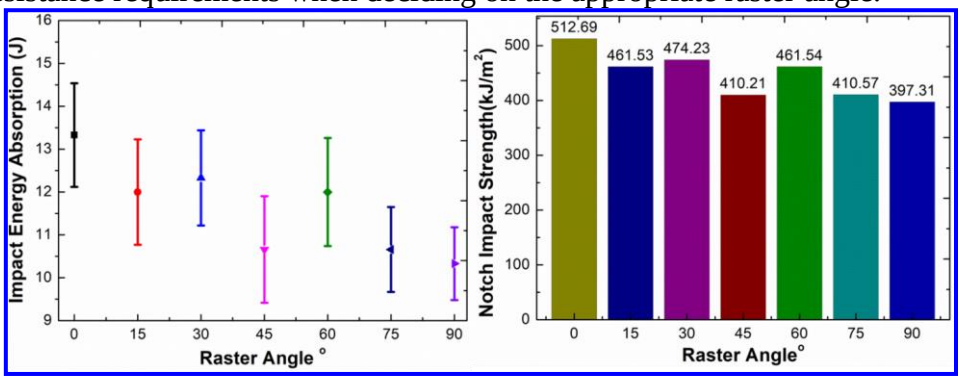

Figure 3: (a) Impact energy absorption and (b) notch impact strength of PLA material with respect to the raster angle under impact test.

Similarly, determined the notch impact strength of the 3D printed PLA specimens and findings are illustrated in Figure 3b. The obtained outcomes from conducting impact tests on PLA samples with different raster angles provide significant insights into the material's response when subjected to dynamic loading circumstances. It is worth mentioning that the PLA sample, which had a raster angle of 0°, had the maximum impact strength, with a notable value of 512.69 kJ/m^2. This finding suggests that when the printing layers are perpendicularly aligned with the direction of impact, PLA has remarkable fracture resistance and is capable of absorbing a significant amount of energy prior to reaching failure. On the contrary, when the raster angle deviates from 0°, a discernible reduction in impact intensity is seen. The impact strength values of raster angles at 15°, 30°, and 60° exhibit a very constant range between 461.53 kJ/m^2 and 474.23 kJ/m^2. Conversely, raster angles of 45°, 75°, and 90° provide lower impact strength values, ranging from 397.31 kJ/m^2 to 410.57 kJ/m^2. The results of this study highlight the need of carefully selecting the angle of the raster in order to maximize the impact resistance of PLA. Specifically, it was shown that a raster angle of 0° resulted in the maximum levels of impact strength and energy absorption. These findings have significant value in engineering applications, particularly when considering the critical aspect of impact performance.

Crack Deflection and Fractography

The reason behind crack nucleation in material is that it needs to release the excessive energy, which is receiving from the external source. Whenever material is absorbing the excessive forces the material is trying to move in the same direction. If any restrictions provided to the material then the material start to deform within its confine region. Once the material reach to peak of plastic deformation then crack nucleation initiate to relive the excessive energy further leads to the physical separation of the material by leaving the crack path. The findings of the impact resistance at each sample raster angle were thoroughly examined with the goal of showing the conditions for the crack propagation in the specimen's shock load-absorbing ability, as shown in Figure 4. From experiment, it found that the zero-degree raster angle exhibited the highest degree of resistance to impact.

The 0° raster angle PLA specimen exhibited intricate fracture characteristics, whereby crack propagation occurred both perpendicular and parallel to the raster angle. This observation indicates the robustness of PLA material in resisting fracture. Porosity was observed by microscopic analysis, as shown by the presence of air gaps. The aforementioned results underscore the impact resistance and energy absorption capabilities of the PLA sample, emphasizing the significance of comprehending these fracture processes in order to enhance the performance of PLA materials. Similarly, a 15° raster angle examination of a PLA sample revealed air gaps, which can act as stress concentration areas, affecting crack initiation and spread. The loading conditions significantly impacted energy dissipation in fracture propagation. Fragmented specimens showed a series of steps, indicating crack initiation. Dispersed particles had a trajectory perpendicular to the raster angle, indicating intricate fracture behavior. Microscopic analysis revealed crack planes and air gaps on the fracture surface. Understanding these processes is crucial for improving the performance of PLA material in impact-prone applications. On the other hand, 30° raster angle fractured sample reveals significant fracture characteristics, resembling previous samples. Fracture growth and energy dissipation were observed, with a zig-zag pattern indicating multiple crack initiation during impact tests. The material showed high resistance to crack propagation, with numerous crack nucleation attempts to impede fracture development. The presence of air gaps in the crack nucleation process was also highlighted. Fractography revealed broken planes and air gaps on the fracture surface, indicating their role in the intricate fracture behavior. The fracture behavior analysis of the 45^{o} raster angle sample revealed that the predominant crack propagation route occurred in the direction of the raster angle. The presence of an air gap had a significant effect in both the initiation and spread of cracks. The presence of an air gap seems to be generating a region of reduced strength, hence facilitating the development of stress concentration. The microscopic images showed a fragmented surface, indicating that the interfacial link between the printed layers exhibited limited effectiveness in absorbing impact energy. In this fractography images shows the crack path through the 60^{o} raster angle sample. The crack propagation followed in zig-zag way it means the crack experienced multiple crack nucleations in the material. Such crack propagation yields better energy absorbing properties. Microscopic images are showing the multiple fractured surfaces, which developed on the different planes. 75^{o} raster angle sample, crack propagated through the material raster angle. Almost one major crack nucleation happened during loading and continued until it fails. It indicating that such material orientation cannot carry the high impact loads during the operation. It seems air gaps were guided the crack propagation and further failure of the specimens. Fractography of the fractured surface displays a plane surface. Additionally, fracture analysis of 90^{o} raster angle sample, material orientation along the applied loading direction seems to be a bad idea why because crack propagation happened in the same direction of the raster angle. Further, crack nucleation occurred once and continued without any resistance to crack propagation in no time. Air gap between the raster also the reason furthers multiple the crack propagation because the strength of the material starts diminishes. It concluded that the material orientation in the direction of the applied load direction never yields the better results.

The fracture occurring at the V-notch location of a specimen during an impact test provides significant information on the mechanism of energy dissipation. The V-notch represents a localized area of stress

concentration, rendering the material more susceptible to the onset of cracks. The deformation behavior of the material is affected by the variation in stress distribution between the V-notch and the impact loading regions. The tensile side undergoes maximum plastic deformation, and the compressive side has comparatively lower plastic deformation. This comprehension aids in the optimization of the material's reaction under varying loading circumstances.

Product Development

After successfully completing the fracture and impact analysis, and manufacturing of the component, the product was designed and developed to serve as curtain tieback. Additionally, the curtain tieback application was further shown, as shown in Figure 5a. In addition, a tailor-made tieback was created in order to fulfill the precise requirements outlined by the customer (see to Figure 5b). The curtain tieback serves as an ideal complement to any window treatment, imparting a sense of elegance and enduring style.

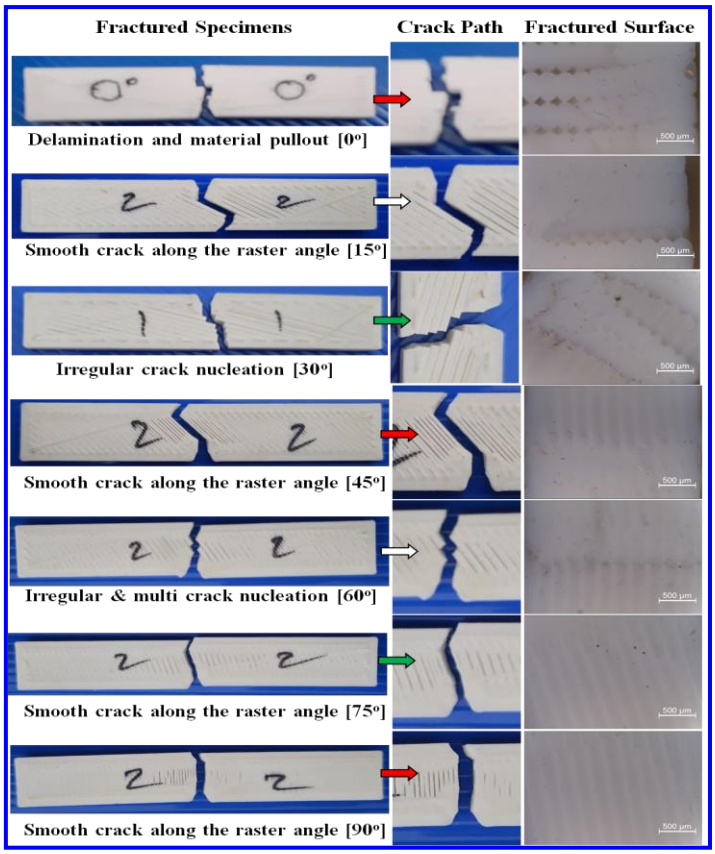

Figure 4: The specimens of PLA were subjected to fracture testing, and the resulting crack propagation and fractured surfaces were analyzed using a microscope. The analysis of the fractography revealed that the fracture had spread across many material planes, hence enhancing the capacity for energy absorption.

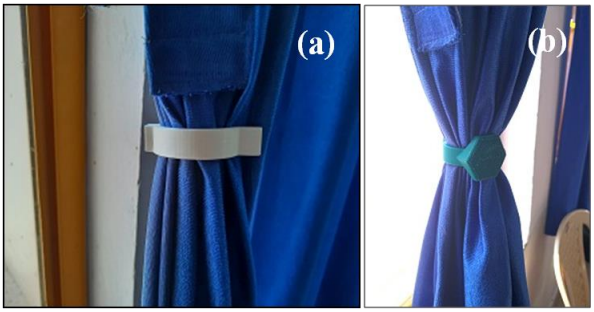

Figure 5: (a) The novel curtain tieback was used to show how to tie back a curtain, and (b) a tailor-made tieback was shown how it might be used.

Conclusion:

Hence, this research adopted the 3D printing technology successfully for the manufacturing of impact testing specimens with varying raster angles from 0^o to 90^o and infill density of the all the impact samples were maintained 100%. Further, printing process parameters were used same for all the samples. As a result, 0^o raster angle sample were exhibited the peak energy absorbing capabilities across the raster angle range (from 0^o to 90^o). It found that the impact strength of the samples mainly depends on the raster angle, which played a key role between the stress intensity and crack propagation phenomenon.

- The 75^o and 90^o raster angle samples exhibited a significant limitation in the form of stress concentration. This stress concentration was further intensified by the produced stress in the sample, resulting in fracture with lower energy consumption compared to other samples. The fracture propagated parallel to the raster angle and encountered no resistance in its route due to the alignment of material orientation and loading direction.
- In the sample, there exists an air gap between each printed bead at different raster angle orientations. The occurrence of crack nucleation led to a discontinuous crack propagation inside the infill pattern, which was effectively impeded. The fracture process was primarily influenced by intense stress because to the limited surface area involved.
- In conclusion, the fracture rate at different raster angle orientations was found to be affected by crack propagation, which was expedited by the existence of a resistant zone within the mesostructure of the specimen.
- In conclusion, the delamination of layers in the mesostructure plays a crucial role in preventing the continuity of crack propagation during impact. In conclusion, the gradual increase in the structure's energy-absorbing ability is a result of the interruption of crack propagation in the fracture region.

The implications of the findings are significant for applications that require high impact resistance and involve the selection of PLA printing orientations. In ending, a raster angle of 0° may be preferred in scenarios where maximizing energy absorption is necessary. It will be important to note that these results will represent a specific set of conditions and may not be universally applicable in the future scope of work. In order to fully comprehend the underlying mechanisms and identify the most effective raster angle for PLA in various situations, additional research and testing will be required in the future.

ORCID iD

Bhimavarapu Sambi Reddy https://orcid.org/0000-0001-9184-0088

References

[1] Memarzadeh, A; Safaei, B.; Tabak, A.; Sahmani, S.; Kizilors, C. Advancements in Additive Manufacturing of Polymer Matrix Composites: A Systematic Review of Techniques and Properties. Materials Today Communications. 2023, 16, 106449.

[2] Mehrpouya, M.; Vosooghnia, A.; Dehghanghadikolaei, A.; Fotovvati, B. The benefits of additive manufacturing for sustainable design and production. InSustainable manufacturing. 2021, 1, 29-59.

[3] Durakovic B. Design for additive manufacturing: Benefits, trends and challenges. Periodicals of Engineering and Natural Sciences. 2018, 6(2), 179-191.

[4] Mohamed, O. A.; Masood, S. H.; Bhowmik, J. L. Optimization of fused deposition modeling process parameters: a review of current research and future prospects. Advances in manufacturing. 2015, 3, 42-53.

[5] Dave H. K.; Patel S. T. Introduction to fused deposition modeling based 3D printing process. Fused deposition modeling based 3D printing. 2021, 1-21.

[6] Taib, N. A.; Rahman, M. R.; Huda, D.; Kuok, K. K.; Hamdan, S.; Bakri, M. K., Julaihi, M. R.; Khan, A. A review on poly lactic acid (PLA) as a biodegradable polymer. Polymer Bulletin. 2023, 80(2), 1179-213.

[7] Barkhad, M.S.; Abu-Jdayil, B.; Mourad, A. H.; Iqbal, M. Z. Thermal insulation and mechanical properties of polylactic acid (PLA) at different processing conditions. Polymers. 2020, 12(9), 2091.
[8] Bakar, A. A.; Zainuddin, M. Z.; Adam, A. N.; Noor, I. S.; Tamchek, N. B.; Alauddin, M. S.; Ghazali, M. I. The study of mechanical properties of poly (lactic) acid PLA-based 3D printed filament under temperature and environmental conditions. Materials Today: Proceedings. 2022, 67, 652-658.
[9] Ambone, T.; Torris, A.; Shanmuganathan, K. Enhancing the mechanical properties of 3D printed polylactic acid using nanocellulose. Polymer Engineering & Science. 2020, 60(8), 1842-1855.
[10] Akhoundi, B.; Behravesh, A.H. Effect of filling pattern on the tensile and flexural mechanical properties of FDM 3D printed products. Experimental Mechanics. 2019, 59, 883-897.
[11] Doshi, M.; Mahale, A.; Singh, S. K.; Deshmukh, S. Printing parameters and materials affecting mechanical properties of FDM-3D printed Parts: Perspective and prospects. Materials Today: Proceedings. 2022, 50, 2269-2275.
[12] Ayatollahi, M. R.; Nabavi-Kivi, A.; Bahrami, B.; Yahya, M. Y.; Khosravani, M. R. The influence of in-plane raster angle on tensile and fracture strengths of 3D-printed PLA specimens. Engineering Fracture Mechanics. 2020, 237, 107225.
[13] Khosravani, M. R.; Soltani, P.; Weinberg, K.; Reinicke, T. Structural integrity of adhesively bonded 3D-printed joints. Polymer Testing. 2021, 100, 107262.
[14] Rajpurohit, S. R.; Dave, H. K. Impact strength of 3D printed PLA using open source FFF-based 3D printer. Progress in Additive Manufacturing. 2021, 6(1), 119-131.
[15] Syrlybayev, D.; Zharylkassyn, B.; Seisekulova, A.; Akhmetov, M.; Perveen, A.; Talamona, D. Optimisation of strength properties of FDM printed parts—A critical review. Polymers. 2021, 13(10), 1587.
[16] Lanzotti, A.; Grasso, M.; Staiano, G.; Martorelli, M. The impact of process parameters on mechanical properties of parts fabricated in PLA with an open-source 3-D printer. Rapid Prototyping Journal. 2015, 21(5), 604-617.
[17] Wang, L.; Gramlich, W. M.; Gardner, D. J. Improving the impact strength of Poly (lactic acid)(PLA) in fused layer modeling (FLM). Polymer. 2017, 114, 242-248.
[18] Zhang, B.; Seong, B.; Nguyen, V.; Byun, D. 3D printing of high-resolution PLA-based structures by hybrid electrohydrodynamic and fused deposition modeling techniques. Journal of Micromechanics and Microengineering. 2016, 26(2), 025015.
[19] Liu, Y.; Bai, W.; Cheng, X.; Tian, J.; Wei, D.; Sun, Y.; Di, P. Effects of printing layer thickness on mechanical properties of 3D-printed custom trays. The Journal of Prosthetic Dentistry. 2021, 126(5), 671-e1.
[20] Mishra, P. K.; Senthil, P.; Adarsh, S.; Anoop, M. S. An investigation to study the combined effect of different infill pattern and infill density on the impact strength of 3D printed polylactic acid parts. Composites Communications. 2021, 24, 100605.